Morphologic patterns associated with *BRCA1* and *BRCA2* genotype in ovarian carcinoma

Robert A Soslow[1], Guangming Han[2], Kay J Park[1], Karuna Garg[1], Narciso Olvera[1], David R Spriggs[3], Noah D Kauff[3,4] and Douglas A Levine[5]

[1]*Department of Pathology, Memorial Sloan-Kettering Cancer Center, New York, NY, USA;* [2]*Department of Pathology and Laboratory Medicine, University of Calgary, Calgary, Alberta, Canada;* [3]*Gynecologic Medical Oncology Service, Department of Medicine, Memorial Sloan-Kettering Cancer Center, New York, NY, USA;* [4]*Clinical Genetics Service, Department of Medicine, Memorial Sloan-Kettering Cancer Center, New York, NY, USA and* [5]*Gynecology Service, Department of Surgery, Memorial Sloan-Kettering Cancer Center, New York, NY, USA*

This study was undertaken with the hypothesis that certain common morphologic features of ovarian carcinomas are predictably associated with *BRCA1* and *BRCA2* deficiencies. We selected 43 high-grade serous carcinomas diagnosed at Memorial Sloan-Kettering Cancer Center that were studied as part of The Cancer Genome Atlas pilot project. In addition to 12 randomly selected nonfamilial *BRCA*-unassociated cases, all 31 Memorial Sloan-Kettering Cancer Center cases with *BRCA1* or *BRCA2* abnormality were included ($n = 43$). Slides were examined to assess tumor architecture, mitotic index, tumor-infiltrating lymphocytes (TILs), nuclear pleomorphism, necrosis, and involvement of fallopian tube epithelium. Comparing *BRCA1*-associated cases (*BRCA1* germline mutation, $n = 4$, *BRCA1* somatic mutation, $n = 6$, *BRCA1* promoter methylation, $n = 13$) with unassociated cases ($n = 12$) identified statistically significant differences in morphology. *BRCA1*-associated high-grade serous carcinomas had more frequent Solid, pseudoEndometrioid, and Transitional cell carcinoma-like morphology (SET features) ($P = 0.0045$), higher mitotic indexes ($P = 0.012$), more TILs ($P = 0.034$), and either geographic or comedo necrosis ($P = 0.034$). *BRCA2*-associated cases (germline mutation, $n = 4$ and somatic mutation, $n = 4$) tended to show SET features, but they were relatively deficient in TILs and necrosis. Two algorithms incorporating tumor architecture, necrosis, and either mitotic indexes or TILs separated cases that showed 2 of 3 features (*BRCA1* associated) from those with 0 of 3 features (*BRCA* unassociated; $P = 0.0016$ and $P = 0.0033$). A test set comprising 9 *BRCA1* germline mutants and 14 high-grade serous carcinoma controls lacking *BRCA1* and *BRCA2* germline mutation was used to validate the algorithms, with specific emphasis on the ability to detect cases with *BRCA1* germline mutation. Best results were obtained with the algorithm that incorporated SET features, necrosis, and mitotic index ($P = 0.0072$; sensitivity of 1.0 (95% CI, 0.66–1.0); specificity of 0.57 (95% CI, 0.29–0.82); positive predictive value of 0.60 (95% CI, 0.32–0.84) and a negative predictive value of 1.0 (95% CI, 0.63–1.0)). These preliminary data indicate potential strong associations between morphology and genotype in high-grade serous carcinomas.
Modern Pathology (2012) **25,** 625–636; doi:10.1038/modpathol.2011.183; published online 23 December 2011

High-grade serous carcinomas of the fallopian tube, ovary, and peritoneum are heterogeneous neoplasms with a variety of morphologic appearances, genotypes, chemosensitivity profiles and prognoses, despite many shared pathologic, clinical, and biologic features. Approximately 30–40% of these carcinomas exhibit *BRCA1* or *BRCA2* inactivation deriving from germline or somatic mutation or from methylation of the *BRCA1* promoter.[1–4] There is now a general consensus that most or perhaps all *BRCA1*-associated adnexal carcinomas are

high-grade serous carcinomas, although the characteristics of *BRCA2*-mutated ovarian cancers are currently not well documented. *BRCA1* inactivation may be associated with relative chemosensitivity[3,4] and favorable prognosis,[5,6] as compared with high-grade serous carcinomas with intact *BRCA1* function, although it is not currently known whether these features are restricted to patients with the best-understood mechanism for *BRCA* inactivation, *BRCA1* germline gene mutation. Inhibitors to poly-ADP ribose polymerase (PARP), which are theoretically more beneficial to patients whose tumors have deficient *BRCA1* or *BRCA2* function, are currently being tested in clinical trials, with positive preliminary results.[7–9] There is mounting clinical interest in predictive biomarkers to identify chemosensitive high-grade serous carcinomas that pursue a relatively favorable clinical course and might be efficiently targeted with PARP inhibitors or related agents. Morphologic criteria at the time of diagnosis would be useful in choice of treatment and patient counseling. Determining which high-grade serous carcinoma patients are more likely than others to harbor germline *BRCA1* or *BRCA2* mutations is also of great interest for selecting patients for genetic testing.

Associations between high-grade serous carcinoma morphology and prognosis and genotype have also been studied, but results are limited. Investigators have documented the relationship between the presence of tumor-infiltrating lymphocytes (TILs) and favorable prognosis,[10–13] and between TILs and *BRCA* status.[13] Nearly as interesting are the classic descriptions of ovarian transitional cell carcinomas, now regarded by many to represent high-grade serous carcinoma variants, with favorable prognosis and relative chemosensitivity.[14–16] We therefore questioned whether these morphologic features were associated with *BRCA1* abnormality, given the associations of each with favorable prognosis and chemosensitivity. Furthermore, solid architecture, nuclear pleomorphism, geographic necrosis, high mitotic index, and TILs have been described in *BRCA1*-associated breast carcinomas.[17–20] This study was undertaken with the hypothesis that routinely assessed morphologic features of ovarian carcinomas are reliably associated with *BRCA1* and *BRCA*2 deficiency states.

Materials and methods

Training Set

We selected 43 HGSCs diagnosed at Memorial Sloan-Kettering Cancer Center (MSKCC) that were studied as part of The Cancer Genome Atlas pilot project.[21] The Cancer Genome Atlas, a multi-institutional effort sponsored by the National Cancer Institute and the National Human Genome Research Institute, catalogs genomic alterations responsible for cancer using high-throughput genome analysis methods. Techniques used include gene expression profiling, copy number assessment, SNP genotyping, genome-wide DNA methylation profiling, microRNA profiling, and whole-exome sequencing. High-grade serous carcinoma is one of the tumor types recently completed by The Cancer Genome Atlas project.[21] Quality control for all The Cancer Genome Atlas specimens is accomplished through a biospecimen core resource to ensure tumor cellularity and nucleic acid integrity.

In addition to 12 randomly selected *BRCA*-unassociated cases, all MSKCC cases with *BRCA* abnormality were included ($n = 31$). All tumors studied were diagnosed at MSKCC as HGSC, based upon Gilks' modification to the WHO criteria for diagnosing high-grade serous carcinoma.[22] Gilks' modification[22] classifies high-grade ovarian carcinomas as high-grade serous carcinoma for cases showing solid, cribriform, microcystic, and transitional cell carcinoma-like architectural patterns as long as confirmatory endometrioid features such as squamous metaplasia, endometrioid adenofibroma, associated endometriosis, and synchronous endometrioid carcinoma of endometrium are absent. There were 4 cases with *BRCA1* germline mutation, 13 cases with *BRCA1* promoter methylation, 6 cases with *BRCA1* somatic mutation, 4 cases with *BRCA2* germline mutation, 4 cases with *BRCA2* somatic mutation, and 12 cases without these abnormalities.

Slides from the MSKCC archives were retrieved after obtaining Internal Review Board approval. The mean number of slides reviewed per case was 10, with the minimum number of slides being 3. Every effort was made to study tumor characteristics in the primary site (ie, fallopian tube and ovary), but omental metastases were studied if slides representing the primary site were not available. All slides were reviewed by one pathologist (RAS) without knowledge of genotype.

Slides were first examined at scanning magnification ($\times 20$) for architectural characterization and the presence of obvious TILs, comedo-like or geographic necrosis (Figure 1), nuclear pleomorphism (Figure 2), and tubal epithelial involvement. The number of TILs per high-power field ($\times 400$; Figure 3) and the mitotic index, expressed as mitoses per 10 high-power fields, were assessed after having identified areas enriched for each characteristic at $\times 20$ magnification (see following), whenever possible.

The following architectural patterns were noted: solid (Figure 4), cribriform/pseudoendometrioid (Figure 5), transitional cell carcinoma-like (Figure 6), papillary (Figure 7), micropapillary (Figure 8), compressed micropapillary (Figure 9), infiltrative papillary (Figure 10), and infiltrative micropapillary (Figure 11). The architectural descriptions of transitional cell carcinoma-like architecture provided by Eichhorn and Young[23] used to categorize these cases were undulating, diffuse, insular, trabecular, 'punched out microspaces' (the
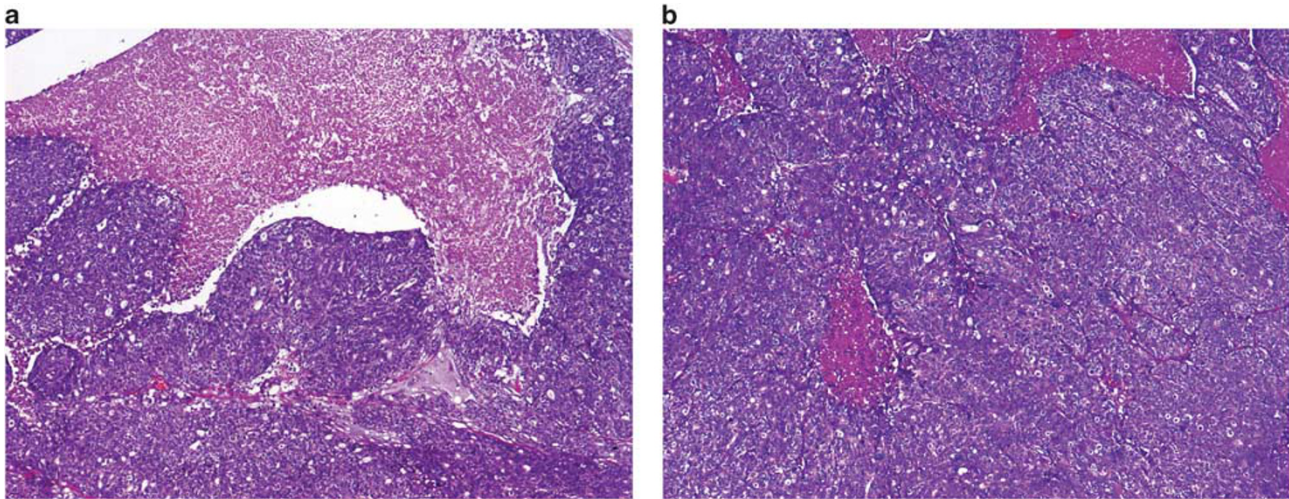
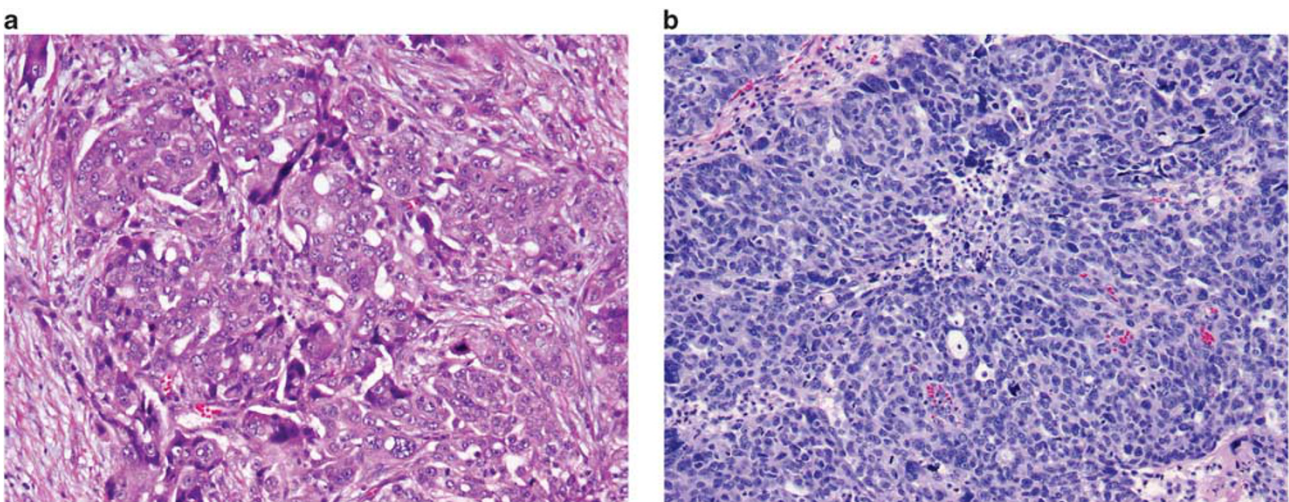**Figure 1** (**a**) Geographic necrosis and (**b**) comedo necrosis.

Figure 2 (**a**, **b**) Nuclear pleomorphism contrasts with areas showing small, uniform tumor cells.
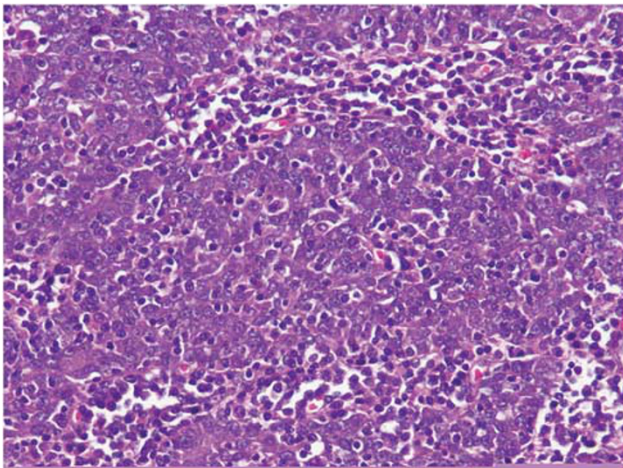

Figure 3 Tumor-infiltrating lymphocytes.

appearance of which overlaps with cribriform and pseudoendometrioid growth patterns), and large blunt papillae. The micropapillary pattern (Figure 8) describes high-grade serous carcinoma with architectural similarity to micropapillary serous borderline tumor (also known as noninvasive low-grade micropapillary serous carcinoma). Compressed micropapillary patterns (Figure 9) were recognized when intermediate-power microscopy was required to distinguish closely spaced micropapillae, sometimes with slit-like spaces between them, from tumors with solid architecture. Tumors with destructive stromal invasion in the form of papillae with fibrovascular support were considered part of the spectrum of infiltrative papillary architecture (Figure 10) and tumors with destructive stromal invasion in the form of micropapillae lacking fibrovascular support were considered to show infiltrative micropapillae (Figure 11). The extent of each pattern was visually estimated by roughly calculating the area involved on each slide of the entire case. Necrosis and nuclear pleomorphism were scored as present when easily appreciated foci were present in the majority of slides reviewed.
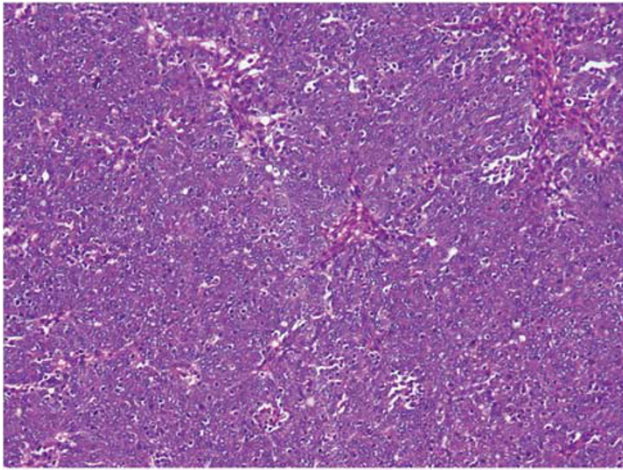
Figure 4 Solid architecture.
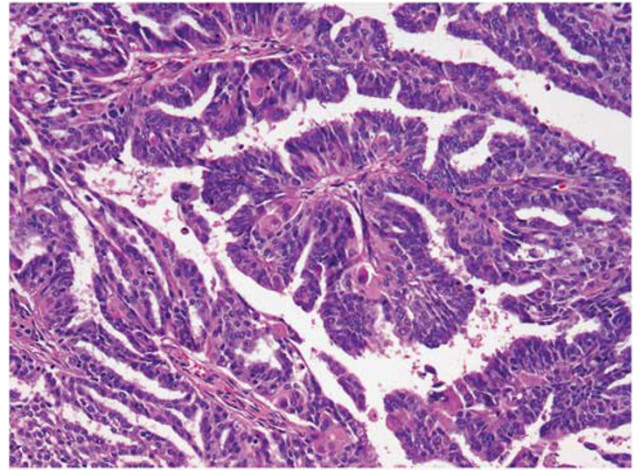
Figure 7 Papillary architecture.
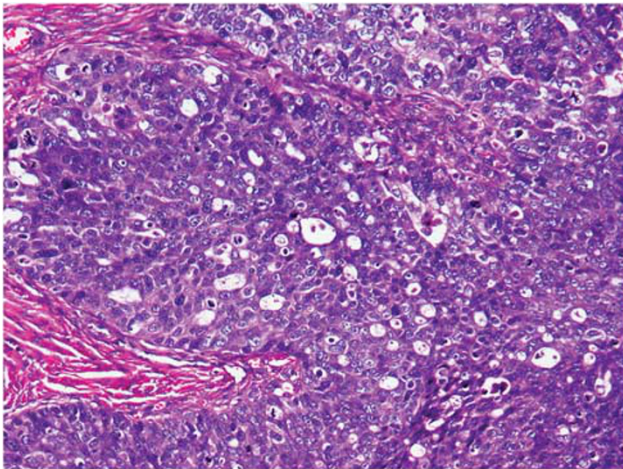
Figure 5 Cribriform/pseudoendometrioid architecture.
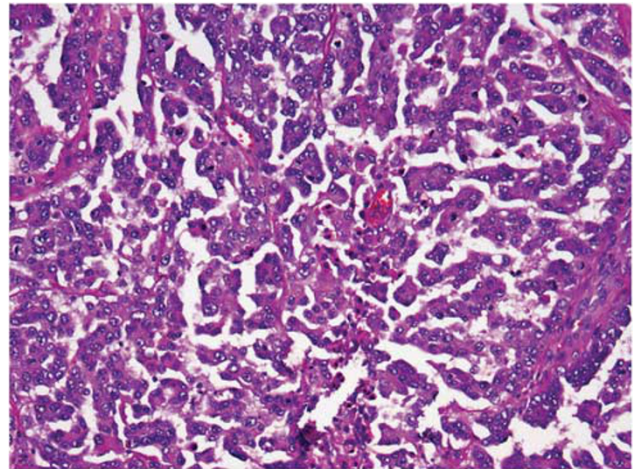
Figure 8 Micropapillary architecture.
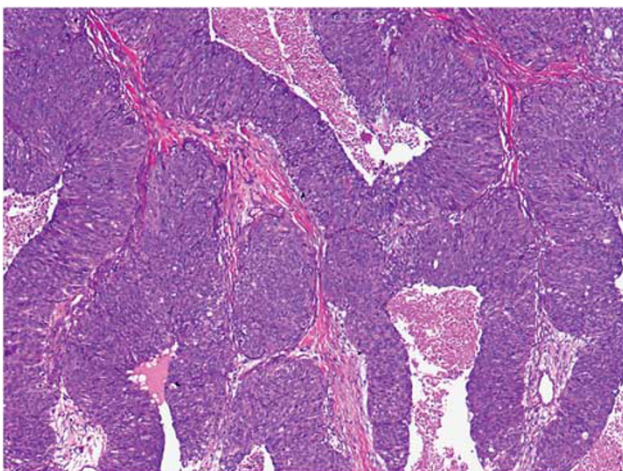
Figure 6 Transitional cell carcinoma-like (transitional cell carcinoma-like) architecture.
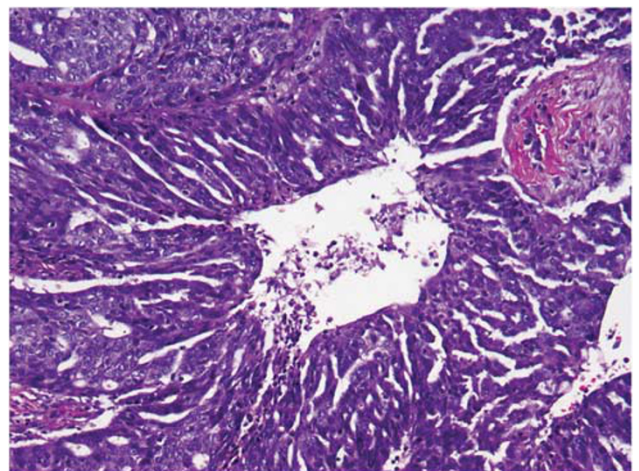
Figure 9 Compressed micropapillae.

TIL and mitotic index counting was performed in areas enriched for each characteristic after having identified hot spots. 'Hot spots' describe areas in which the highest density of TILs or mitotic figures was found at low-power magnification (× 20) after scanning all tumor slides, although it is acknowl-

Figure 10 Infiltrative papillae.

Figure 11 Infiltrative micropapillae.

edged that it was sometimes difficult to detect hot spots in cases with diffusely distributed dense TILs and high mitotic indexes or tiny hot spots in a tumor with abundant mixed acute and chronic inflammatory infiltrates that was otherwise deficient in dense TILs. Efforts at identifying hot spots revealed at least three patterns of TIL distribution: (1) diffusel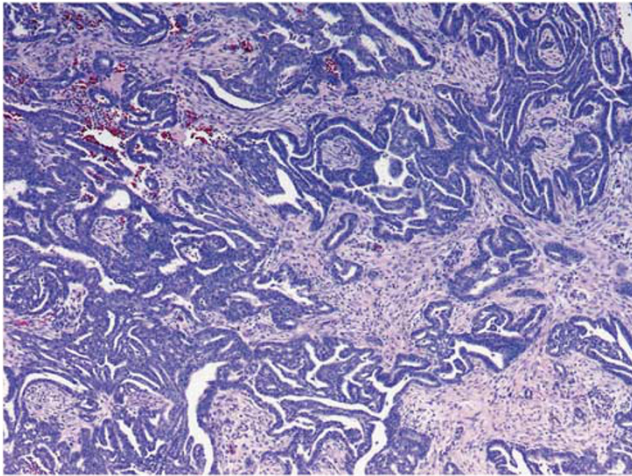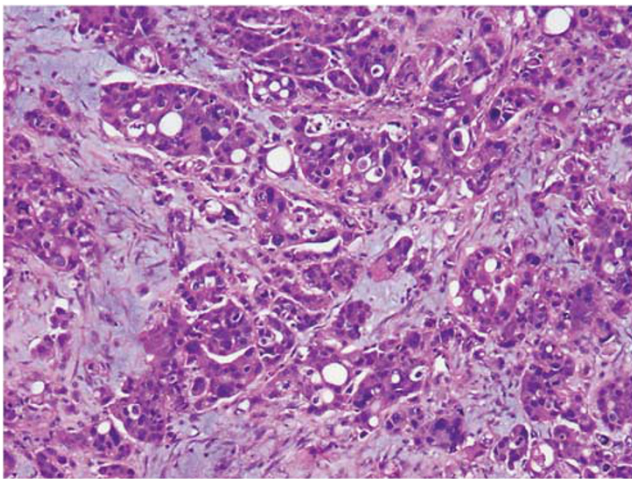y dense TILs in the primary site; (2) focal TIL hot spots in a background of a TIL-poor tumor in the primary site; and (3) focal TIL hot spots most obvious in metastatic locations. For TILs, care was taken to count only intercellular lymphocytes, not lymphocytes within blood vessels or at the periphery of tumor nests. Fallopian tube epithelial involvement in the form of either serous tubal intraepithelial carcinoma or invasive high-grade serous carcinoma was scored only when sections of fimbria were available for review. Including cases without representation of fimbria might have compromised our ability to detect whether these putative precursors of high-grade serous carcinoma, usually localized to the distal one-third of the fallopian tube, including

the fimbria, are differentially distributed in cases with and without mutations.

Preliminary data were then correlated with genotype. The distribution of solid, cribriform, and transitional cell carcinoma-like patterns overlapped significantly, and hence they were collapsed into one value, SET features ('Solid, pseudoEndometrioid and/or Transitional cell carcinoma-like') for subsequent calculations. Cases showing more than 25% SET features were coded as showing SET features. When more than one SET pattern was identified, the percentage values were added together. For example, if a tumor showed 20% solid architecture and 10% pseudoendometrioid architecture, the SET value was 30% and the case was coded as SET-like. The data for *BRCA1* germline and somatic mutations were combined with those of the *BRCA1* promoter methylation groups for subsequent calculations involving the training set because of relative paucity of the former cases and substantial morphologic overlap between these groups. We use the term '*BRCA1*-associated' to distinguish these from cases lacking *BRCA1* and *BRCA2* abnormalities (ie, '*BRCA*-unassociated' cases).

Statistical Methods

Prevalence of morphologic features was compared between the 23 cases with germline or somatic *BRCA1* inactivation (including somatic mutation and promoter methylation) with the 12 *BRCA*-unassociated cases. Categorical values were compared using Fisher's exact test (two tailed) and continuous variables were compared using Mann–Whitney test (two tailed). All statistical analyses were performed using GraphPad Prism software. Given the small number of case with *BRCA2* inactivation, qualitative differences between cases with *BRCA2* inactivation and both *BRCA1*-associated and *BRCA*-unassociated cases are described, but formal statistical testing was not performed.

Algorithm Construction

Morphologic features that were statistically different between the *BRCA1*-associated cases and the *BRCA*-unassociated cases were used to construct two algorithms that might be useful for routine diagnostic work. Each algorithm was constructed with three variables and scored a tumor as *BRCA1* related if ≥ 2 features were present. Cases lacking any features were scored as *BRCA* unrelated and cases showing only one feature were considered indeterminate.

Test Set

Validation of the algorithms was then attempted using 23 additional serous ovarian cancer cases not included in The Cancer Genome Atlas that were

Table 1 Summary of morphologic characteristics of the training set organized by genotype

	Tumor-infiltrating lymphocytes per high-power field, median (range)	Mitotic index, median (range)	Solid, pseudoendometrioid, and transitional cell carcinoma-like (SET) features	Necrosis	Nuclear pleomorphism	Fallopian tube involvement
BRCA1 germline (n = 4)	31 (10–69)	52 (40–71)	2/4	3/4	2/4	1/1
BRCA1 somatic (n = 6)	29 (5–62)	64 (19–105)	4/6	3/6	3/6	5/5
BRCA1 methylated (n = 13)	52 (13–88)	60 (17–102)	10/13	7/13	7/13	4/5
BRCA2 germline (n = 4)	19 (5–43)	62 (8–126)	4/4	4/4	4/4	3/3
BRCA2 somatic (n = 4)	16 (12–60)	35 (12–60)	2/4	0/4	3/4	2/2
BRCA unassociated (n = 12)	29 (2–140)[b]	37 (15–94)	2/12	2/12	3/12	6/10
P-value[a]	0.034[b]	0.012[b]	0.0045	0.034	0.16	0.65
Overall (n = 43)	36 (mean) 29 (median)	53 (mean) 51 (median)	24/43	19/43	21/43	21/26

[a]Based on comparisons between BRCA1-associated and unassociated cases.

[b]The P-values for tumor-infiltrating lymphocytes and mitotic indexes were calculated from categorical values, with values above the median being considered 'positive.' The P-values for tumor-infiltrating lymphocytes and mitotic indexes as continuous variables were 0.43 and 0.030, respectively.

'Solid, pseudoendometrioid, and transitional cell carcinoma-like' includes classically described transitional cell carcinoma-associated patterns as well as associated solid and cribriform (pseudoendometrioid) patterns (Figures 4–6). Cases showing >25% SET were coded as showing SET features.

characterized for germline BRCA status. After excluding one case with BRCA2 germline mutation, cases with and without BRCA1 germline mutations (n = 9 and 14, respectively) were selected from sequential patients who underwent genetic testing as part of clinical care at Memorial Sloan-Kettering Cancer Center between 2008 and 2010 (BRCA1 associated, n = 9; BRCA unassociated, n = 14). Although all of the control case were BRCA1 wild type, it was not known whether any of these cases had BRCA1 somatic mutation, a BRCA2 somatic mutation, or methylation of the BRCA1 promoter. The mean number of slides reviewed per case in the validation set was eight, with the minimum number of slides reviewed being three. Sensitivity, specificity, positive predictive value, and negative predictive value of the algorithms were calculated using two-tailed Fisher's exact test.

Results

Table 1 displays a summary of morphologic characteristics of the training set organized by genotype.

Morphologic Features of the Training Set

Table 2 displays the distribution of architectural patterns. Of 43 cases, 8 displayed only one growth pattern (ie, a homogeneous architectural growth pattern), which was seen more commonly in BRCA-associated cases as compared with BRCA-unassociated cases. Of the 8 architecturally homogeneous cases, 7 were captured as uniformly SET in appearance (Figures 4–6). The remaining 35 cases were architecturally heterogeneous, all showing more than one growth pattern, with 8 of them showing at least 3

distinct patterns. Although patterns found in tumors from the primary site were evaluated primarily whenever possible, we noted significant morphological heterogeneity when comparing features in primary and metastatic sites. Features found more commonly in metastatic sites included infiltrative patterns with stromal desmoplasia and lymphocyte-rich, mixed inflammatory infiltrates at the advancing edge of infiltrative tumor nests.

The distribution of TILs (Figure 3) was also found to be relatively homogeneous in BRCA1-associated cases (pattern 1 described in Materials and Methods), whereas it tended to be heterogeneous in unassociated cases (pattern 2 described in Materials and Methods). TILs were seldom prominent at low-power inspection of primary site tumors in BRCA-unassociated cases, although hot spots could be appreciated with effort, particularly in extraovarian sites when slides representing ovary or fallopian tube contained only minimal tumor (pattern 3 described in Materials and Methods). Median TIL counts in cases with diffusely distributed TILs were 37 per high-power field.

Cases displaying obvious nuclear pleomorphism at scanning magnification contained islands of large cells, sometimes with abundant eosinophilic cytoplasm, and highly irregular nuclei, either vesicular with macronucleoli, or hyperchromatic with bizarre and convoluted nuclear forms. Psammoma bodies were less frequently seen in cases with BRCA1 abnormality (9/23 vs 10/12).

BRCA1-Associated Cases

Statistically significant associations were found between BRCA1-associated abnormality and SET

Table 2 Architectural patterns in the training set

Case no.	Genotype	Primary pattern	Secondary pattern	Tertiary pattern
1	BRCA1 germline	Solid (50%)	Papillary (50%)	
2[a]	BRCA1 germline	Transitional cell carcinoma (30%)	Solid (10%)	Infiltrating MP (10%)
3	BRCA1 germline	Papillary (100%)		
4	BRCA1 germline	Papillary (80%)	Infiltrating MP (15%)	Solid (5%)
5	BRCA1 methylated	Papillary (50%)	Infiltrating papillary (50%)	
6[a]	BRCA1 methylated	Papillary (50%)	Cribriform (25%)	Solid (10%)
7	BRCA1 methylated	Cribriform (70%)	Solid (30%)	
8	BRCA1 methylated	Infiltrating MP (50%)	Cribriform (25%)	Solid (25%)
9	BRCA1 methylated	Transitional cell carcinoma (100%)		
10	BRCA1 methylated	Papillary (60%)	MP (35%	Solid (5%)
11	BRCA1 methylated	Transitional cell carcinoma (100%)		
12	BRCA1 methylated	Solid (100%)		
13	BRCA1 methylated	Solid (50%)	Microcystic (50%)	
14	BRCA1 methylated	Solid (50%)	Transitional cell carcinoma (50%)	
15	BRCA1 methylated	Papillary (80%)	Solid (20%)	
16	BRCA1 methylated	Papillary (60%)	Solid (30%)	MP (10%)
17	BRCA1 methylated	Papillary (80%)	MP (15%)	Solid (5%)
18	BRCA1 somatic	Papillary (90%)	Solid (10%)	
19	BRCA1 somatic	Papillary (50%)	Transitional cell carcinoma (50%)	
20	BRCA1 somatic	Transitional cell carcinoma (100%)		
21	BRCA1 somatic	Solid (75%)	Cribriform (25%)	
22	BRCA1 somatic	Infiltrating MP (80%)	MP (20%)	
23	BRCA1 somatic	Solid (75%)	Cribriform (25%)	
24	BRCA2 germline	Transitional cell carcinoma (100%)		
25	BRCA2 germline	Infiltrating MP (100%)		
26	BRCA2 germline	Papillary (95%)	Solid (5%)	
27	BRCA2 germline	Transitional cell carcinoma (100%)		
28	BRCA2 somatic	Papillary (75%)	Infiltrating MP (25%)	
29	BRCA2 somatic	Infiltrating papillary (50%)	Infiltrating MP (50%)	
30	BRCA2 somatic	Papillary (50%)	Solid (50%)	
31	BRCA2 somatic	Solid (70%)	Transitional cell carcinoma (30%)	
32	BRCA unassociated	Infiltrating papillary (50%)	Infiltrating MP (50%)	
33	BRCA unassociated	Papillary (60%)	MP (30%)	Solid (10%)
34	BRCA unassociated	Papillary (95%)	Solid (5%)	
35	BRCA unassociated	Papillary (90%)	Solid (10%)	
36	BRCA unassociated	Papillary (45%)	MP (40%)	Solid (15%)
37	BRCA unassociated	Infiltrating MP (50%)	Papillary (50%)	
38	BRCA unassociated	Infiltrating papillary (50%)	Infiltrating MP (50%)	
39	BRCA unassociated	Infiltrating papillary (60%)	Infiltrating MP (35%)	Solid (5%)
40	BRCA unassociated	Papillary (65%)	Infiltrating papillary (25%)	Solid (10%)
41	BRCA unassociated	Papillary (50%)	Cribriform (25%)	Transitional cell carcinoma (25%)
42	BRCA unassociated	Transitional cell carcinoma (100%)		
43	BRCA unassociated	Papillary (90%)	Solid (10%)	

[a]Quaternary and quinary patterns were also present.

features ($P = 0.0045$; Figures 4–6). Analyzing mitotic rate as a continuous variable indicated that cases with BRCA1-associated abnormality had higher mitotic indexes than other cases ($P = 0.030$). When mitotic index was evaluated as categorical values split at the median (51), the positive association between mitotic index and BRCA1 abnormality remained significant ($P = 0.012$). Necrosis (Figure 1) was also positively associated with BRCA1 abnormality ($P = 0.034$). The TIL count was not significantly different between groups ($P = 0.43$), although it should be noted that the highest TIL counts were seen in cases with BRCA1 promoter methylation, where the median TILs count (52 per high-power field) significantly exceeded the median overall (29 per high-power field) and the median counts seen in every other group. When cases showing only focally increased TILs were excluded (patterns 2 and 3 described in Materials and Methods), and TILs evaluated as categorical values split at the median (29 per high-power field), then the positive association between TILs and BRCA1 abnormality was significant ($P = 0.034$). Fallopian tube epithelial involvement was more frequently found in BRCA1-associated cases, but the prevalence, 9 of 10, was not significantly different from that seen in BRCA1-unassociated cases (6 of 10).

BRCA2-Associated Cases

Only eight BRCA2-associated cases were studied, four with germline mutations and four with somatic mutations. Statistical analyses were therefore not performed. However, it is notable that although these tumors as a group had a tendency to exhibit SET features (5/8 cases), none of the cases with BRCA2 somatic mutation showed geographic necrosis
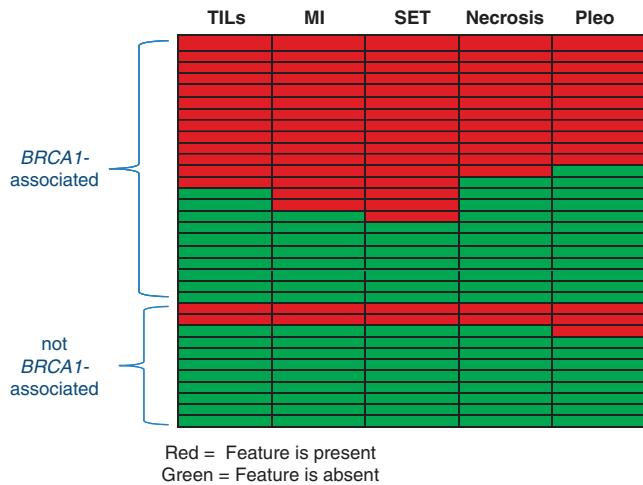
Figure 12 Heatmap showing distribution of morphologic features by genotype. Tumor-infiltrating lymphocytes, high mitotic index, solid, pseudoendometrioid, and transitional cell carcinoma-like features, pleomorphism, and necrosis are seen more frequently in *BRCA1*-associated cases. Green indicates feature not present, and red indicates feature present. Excluding the column indicating tubal involvement, which was not found to be discriminatory, yields a pattern with robust representation of variables (high density of red boxes; low density of green boxes) in *BRCA1*-associated cases when compared with cases lacking *BRCA-1* association (low density of red boxes; high density of green boxes). TILs: tumor-infiltrating lymphocytes >29/high-power field and diffusely distributed; MI: >51 mitotic figures per 10 high-power fields; SET: solid, pseudoendometrioid and/or transitional cell carcinoma-like architectural features in >25% of tumors; Pleo: pleomorphism appreciable at scanning magnification in >25% of tumors; Tubal: high-grade serous carcinoma involves tubal epithelium, including serous tubal intraepithelial carcinoma; Necrosis: necrosis appreciable at scanning magnification in >25% of tumors; *BRCA1*-associated includes cases with germline or somatic mutation or *BRCA1* promoter methylation.

or TIL counts that exceeded the median. All evaluable cases showed involvement of fallopian tube epithelium.

Algorithm

The distribution of features seen in each case is displayed in a heatmap (Figure 12). The four variables showing statistically significant differences between *BRCA1*-associated and *BRCA*-unassociated tumors were used to devise two algorithms, each with three variables. Features evaluated in the first algorithm included SET appearance, necrosis, and diffusely distributed TILs that exceeded the median (>37 TILs in one high-power field). In the second algorithm, TILs were replaced with mitotic index (mitotic index that exceeded the median (>51 mitotic figures per 10 high-power field)). The algorithms scored a tumor as *BRCA* related if ≥2 features were present. Cases lacking any features were scored as *BRCA* unrelated and cases showing only one feature were considered indeterminate. Tables 3 and 4 display the distribution of cases from The Cancer Genome Atlas set with and without

Table 3 Distribution of solid, pseudoendometrioid, and transitional cell carcinoma-like (SET) features, necrosis, and tumor-infiltrating lymphocytes (algorithm 1)

	No features	One feature	Two features	Three features
BRCA1 germline (n = 4)	0	2	1[a]	1[a]
BRCA1 somatic (n = 6)	2	0	2[b]	2[b]
BRCA1 methylated (n = 13)	1	3[b]	6[c]	3[d]
BRCA unassociated (n = 12)	5	5	1[a]	1[a]

[a]One case with SET features.
[b]Two cases with SET features.
[c]Five cases with SET features.
[d]Three cases with SET features.
This algorithm was tested to determine whether *BRCA1* association could be predicted by the presence of two or three variables: SET features, tumor-infiltrating lymphocytes, and necrosis. The comparison group comprises cases without solid, pseudoendometrioid, and transitional cell carcinoma-like features, tumor-infiltrating lymphocytes, or necrosis. The 'one feature' column indicated cases indeterminate for *BRCA1* association based on the presence of only one variable.

Table 4 Distribution of solid, pseudoendometrioid, and transitional cell carcinoma-like (SET) features, necrosis, and mitotic index (algorithm 2)

	No features	One feature	Two features	Three features
BRCA1 germline (n = 4)	0	1	2[a]	1[a]
BRCA1 somatic (n = 6)	1	1	1[a]	3[b]
BRCA1 methylated (n = 13)	1	2[a]	8[c]	2[d]
BRCA unassociated (n = 12)	5	5	2[d]	0

[a]One case with SET features.
[b]Three cases with SET features.
[c]Seven cases with SET features.
[d]Two cases with SET features.
This algorithm was tested to determine whether *BRCA1* association could be predicted by the presence of two or three variables: solid, pseudoendometrioid, and transitional cell carcinoma-like features, mitotic index, and necrosis. The comparison group comprises cases without solid, pseudoendometrioid, and transitional cell carcinoma-like features, mitotic index, or necrosis. The 'one feature' column indicates cases indeterminate for *BRCA1* association based on the presence of only one variable.

BRCA1 abnormality when characterized according to each of these two algorithms.

Of 23 informative cases, 15 met *BRCA1*-associated criteria in algorithm 1, as compared with 2 of 12 informative cases without *BRCA1* abnormality (P = 0.012). The sensitivity of the algorithm was 88% (95% CI, 0.64–0.99) and the specificity was 56% (95% CI, 0.31–0.78). Of 23 cases, 17 met *BRCA1*-associated criteria in algorithm 2, as com-
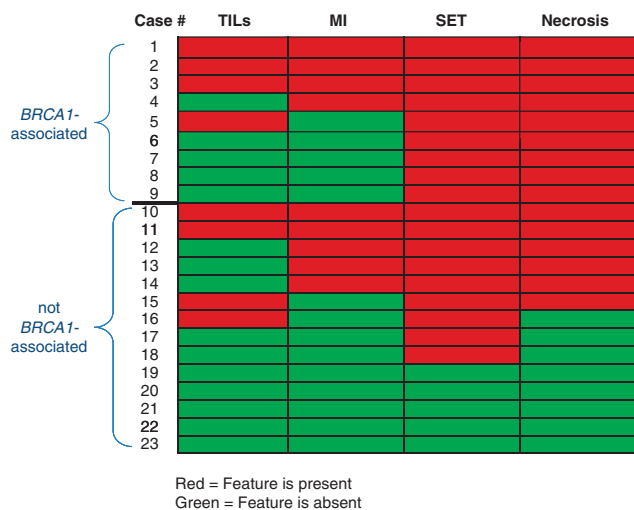
Figure 13 Heatmap of test set showing distribution of morphologic features by genotype.

pared with 2 of 12 informative cases without *BRCA1* abnormality ($P = 0.0033$). The sensitivity of this algorithm was 89% (95% CI, 0.67–0.99) and the specificity was 63% (95% CI, 0.35–0.85).

Test Set

We were able to assemble a modest number of cases to attempt validation of these algorithms, with focus on *BRCA1* germline mutation. The test set included cases with and without known *BRCA1* germline mutation ($n = 9$ and 14, respectively) (Figure 13). Although none of the cases in the test set had a germline *BRCA2* mutation, unlike the learning set, it was not known whether these cases had *BRCA1* somatic mutation, a *BRCA2* somatic mutation, or methylation of the *BRCA1* promoter. As previously, cases with 2 or 3 features present were scored as 'predictive of *BRCA1*.' In one calculation, cases with 0 or 1 criterion were scored as 'not predictive of *BRCA1*' and in a subsequent calculation, only cases with 0 features were scored as 'not predictive of *BRCA1*.' Cases with only one criterion were not included in the second calculation because they were deemed 'indeterminate' in the learning set.

In the first algorithm, including SET features, necrosis, and TILs, all 9 *BRCA1* germline mutants showed features predictive of *BRCA1*; 4 cases showed all 3 features and 5 showed 2 features. This contrasted with the BRCA controls, of which 7 of 14 showed features predictive of *BRCA1* (3 cases with 3 features and 4 cases with 2 features) and 7 cases showed only 1 feature, such as SET ($n = 2$), or none ($n = 5$). In the second algorithm, including SET features, necrosis, and mitotic index, all 9 *BRCA1* germline mutants showed features predictive of *BRCA1*; 4 cases showed all 3 features and 5 showed 2 features. This contrasted with the BRCA controls, of which 6 of 14 showed features predictive of

BRCA1 (5 cases with 3 features and 1 case with 2 features) and 8 cases showed only 1 feature, such as SET ($n = 3$), or none ($n = 5$).

The first algorithm predicted *BRCA1* association markedly better than chance; $P = 0.019$ scoring cases with 0 or 1 feature as 'not predictive of *BRCA1*' and $P = 0.045$ using the second calculation that omitted cases with only 1 feature. Calculations that considered cases with 0 or 1 feature as 'not predictive of *BRCA1*' yielded a sensitivity of 1.0 (95% CI, 0.66–1.0); specificity of 0.50 (95% CI, 0.23–0.77); positive predictive value of 0.56 (95% CI, 0.30–0.80); and a negative predictive value of 1.0 (95% CI, 0.59–1.0). Calculations that omitted cases with only one feature yielded a sensitivity of 1.0 (95% CI, 0.66–1.0); specificity of 0.42 (95% CI, 0.15–0.72); positive predictive value of 0.56 (95% CI, 0.30–0.80); and a negative predictive value of 1.0 (95% CI, 0.48–1.0).

The second algorithm yielded statistically significant results; $P = 0.0072$ scoring cases with 0 or 1 feature as 'not predictive of BRCA1' and $P = 0.038$ using the second calculation that omitted cases with only 1 feature. Calculations that considered cases with 0 or 1 feature as 'not predictive of BRCA1' yielded a sensitivity of 1.0 (95% CI, 0.66–1.0); specificity of 0.57 (95% CI, 0.29–0.82); positive predictive value of 0.60 (95% CI, 0.32–0.84); and a negative predictive value of 1.0 (95% CI, 0.63–1.0). Calculations that omitted cases with only one feature yielded a sensitivity of 1.0 (95% CI, 0.66–1.0); specificity of 0.45 (95% CI, 0.17–0.77); positive predictive value of 0.60 (95% CI, 0.32–0.84); and a negative predictive value of 1.0 (95% CI, 0.48–1.0).

Discussion

Comparatively little is known about relationships between high-grade serous carcinoma morphology and genotype. Although most *BRCA1* germline mutation-associated ovarian carcinomas have been reported to be high-grade serous carcinomas, a relatively small number has been diagnosed as undifferentiated, high-grade endometrioid, mixed epithelial, or mucinous.[24–26] Among the cases categorized as high-grade serous carcinomas, TILs (particularly CD8-positive T cells) have been recognized as characteristic only recently.[13] Little or nothing is currently known about the morphology of high-grade serous carcinomas with *BRCA1* somatic mutations, *BRCA1* promoter methylation, *BRCA2* germline mutations,[27] or *BRCA2* somatic mutations.

Our findings indicate a characteristic morphologic appearance of HGSCs with *BRCA1* abnormality. As compared with cases lacking *BRCA* abnormalities, the former cases are significantly more frequently SET in appearance, contain necrosis and more TILs, and have a higher mitotic index. Obvious pleomorphism was a characteristic feature of

BRCA abnormality, although it did not reach statistical significance. Similar morphological patterns have been described as well in *BRCA1*-associated triple-negative breast carcinomas, including those with a medullary or atypical medullary-like appearance.[17–20] HGSCs with *BRCA* abnormality are also more frequently morphologically homogeneous (ie, show SET features uniformly throughout the tumor and uniformly distributed TILs) as compared with other cases, in which combinations of architectural patterns were more common.

Substantial intratumoral heterogeneity complicated derivation of criteria that might be useful in clinical practice. The extent of transitional cell carcinoma-like features, pleomorphism, and necrosis was empirically derived for segregation into 'positive' and 'negative' cases based on visual estimation, whereas 'positive' TILs and mitotic index were initially scored based on a value that exceeded the median. Because of the observation that TIL distribution tended to be homogeneous in *BRCA*-associated cases and heterogeneous in unassociated cases, only cases with diffusely distributed TILs with more than the median TILs per high-power field were considered TIL positive in construction of the first algorithm, as discussed subsequently. Although additional studies will be necessary to validate these specific numbers, we are confident that tumors with *BRCA*-associated abnormalities do show significantly increased TILs and mitotic indexes relative to other high-grade serous carcinomas. Another complicating factor was the frequent presence of morphological patterns and TILs in peritoneal metastases that were not present in the primary site. Analyses were restricted to primary site tumors and our statistically significant findings support that practice. It is possible that increased TILs in *BRCA1*-unassociated cases and in metastatic sites are B cells or non-CD8-positive T cells.

We explored the application of two algorithms that took into account multiple morphological features because evaluation of only one feature for categorization into *BRCA1*-associated or -unassociated groups suggested this approach would be insufficient for diagnostic testing. The algorithms, devised from the learning set, separated cases showing two or three characteristic features from those with only one feature or none. Despite the apparent strengths of the algorithms, we found 2 of 12 *BRCA1*-unassociated cases from the training set that met criteria in both algorithms tested. It is possible that such cases represent examples of homologous recombination deficiency unrelated to specific alterations of *BRCA1* or *BRCA2*. Homologous recombination refers to one of several mechanisms for the repair of deleterious double-strand DNA breaks. Both *BRCA1* and *BRCA2* gene products can accomplish this type of repair; however, there are a number of other pathways that can theoretically lead to homologous recombination. The two cases with morphologic appearances consistent with *BRCA* dysfunction without known *BRCA* defects may represent tumors containing a separate mechanism leading to homologous recombination deficiency.

We attempted to validate these algorithms in a relatively small test set with particular focus on the ability to detect cases with *BRCA1* germline mutation. The strongest results derived from use of the second algorithm, which accounted for SET features, necrosis, and mitotic index. These results should be interpreted in the context of current clinical practice and knowledge regarding the prevalence of *BRCA* abnormalities in unselected cohorts of high-grade serous carcinoma patients. Results from The Cancer Genome Atlas indicate that as many as 50% of high-grade serous carcinomas may have abnormalities in the homologous recombination pathway, with ~20% having germline or somatic mutations in *BRCA1* or *BRCA2* somatic mutations; 11% having *BRCA1* promotor methylation; and an additional 20% having other abnormalities such as *EMSY* amplification or mutation, *PTEN* deletion, or mutations in one of the Fanconi Anemia genes.[21] Detecting which patients have an inherited predisposition to breast and ovarian cancer typically centers on diagnosis of high-grade serous carcinoma, family history, and referral for genetic testing. Excluding SET pattern tumors from the family of high-grade serous carcinoma might prevent affected patients from eligibility for screening programs. In most centers, selection for genetic testing is individualized, although genetic testing is increasingly being offered to all high-grade serous carcinoma patients in some centers, including Memorial Sloan-Kettering Cancer Center. This approach assumes a pretest probability of *BRCA1* mutation of ~16–17%, resulting in testing 6 patients to detect 1 with a germline *BRCA1* mutation. The theoretical practical benefit of our algorithms is that because of very high negative predictive values, they exclude up to one-third of patients from the need for genetic testing, although careful evaluation of the family history remains imperative to minimize false negatives.

The data suggest that the algorithms significantly enrich the pool of patients to be tested by increasing the positive predictive value from that expected by chance (16–17%) to as high as 60%, although it is acknowledged that the test set overrepresents the prevalence of *BRCA1* germline mutations. We know from the training set that SET features, necrosis, high mitotic index, and dense TILs are not restricted to tumors with *BRCA1* germline mutation, such that some of the 50% of tumors meeting criteria but lacking *BRCA1* germline mutation will show instead *BRCA1* somatic mutation, *BRCA1* promoter methylation, *BRCA2* somatic mutation, or, possibly, other homologous recombination abnormalities. It is unknown if the clinical features of high-grade serous carcinomas associated with *BRCA1* germline mutation can be extrapolated to these different genomic settings.

BRCA1 and BRCA2 morphologic patterns
RA Soslow et al
635

The presence of SET patterns theoretically accounts for previous reports of high-grade endometrioid, transitional cell carcinoma, and undifferentiated carcinomas in *BRCA1* germline cases.[28–30] Whether tumors exhibiting these architectural patterns should be classified as high-grade serous carcinoma is controversial. Immunohistochemical data demonstrate that tumors reported as ovarian transitional cell carcinomas are not only immunophenotypically dissimilar from urothelial carcinomas of the urinary tract, but also express WT1 at rates that are nearly identical to typical high-grade serous carcinoma.[31] Furthermore, the classical description of ovarian transitional cell carcinomas, provided by Eichhorn and Young,[23] includes tumors with foci that are indistinguishable from high-grade serous carcinomas. Immunohistochemical data linking pseudoendometrioid tumors to high-grade serous carcinomas are currently lacking, but gene expression data indicate that most so-called 'high-grade ovarian endometrioid adenocarcinomas' have profiles that both overlap with high-grade serous carcinomas and vary significantly from low-grade ovarian endometrioid adenocarcinomas.[32] The groups from Memorial Sloan-Kettering Cancer Center[33] and Vancouver General Hospital[22] have argued in favor of subsuming SET tumors into the high-grade serous carcinoma family, and investigators have demonstrated both improved diagnostic reproducibility and the clinical relevance of this practice.[22,34] Revised Gynecologic Oncology Group criteria now regard SET tumors as high-grade serous carcinoma. Considering SET tumors as high-grade serous carcinoma variants also strongly anchors these tumors into the family of high-grade serous carcinomas, which may trigger genetic testing for *BRCA* abnormality. Nonetheless, we do believe that SET tumors are biologically and clinically distinctive, such that it is reasonable to call attention to their existence in diagnostic reporting (ie, high-grade serous carcinoma, transitional cell carcinoma-like variant).

The number of *BRCA1* mutation cases in the training set was too small to detect differences between them and cases with *BRCA1* promoter methylation. Similarly, the number of cases with *BRCA2* abnormality was limited in this series, but we can make some qualitative observations. Cases with *BRCA1* promotor methylation had among the highest TIL counts and frequently showed SET features and high mitotic indexes. *BRCA2* germline mutated cases had morphological features that overlapped with the *BRCA1* group, including SET features, pleomorphism, and necrosis, although they less frequently showed high numbers of TILs. *BRCA2* somatically mutated cases tended to lack TILs and necrosis, although they also retained the characteristic architecture and pleomorphism seen in *BRCA1* cases.

In summary, we have demonstrated very strong correlations between genotype and high-grade serous carcinoma phenotype. Tumors lacking the characteristic histological features described herein are quite unlikely to be associated with *BRCA1* abnormality. Once validated, these data may potentially be exploited to narrow the pool of high-grade serous carcinoma patients tested for germline mutations. The data also allow for recognition of tumors with potentially favorable clinical profiles that might be targeted with specific therapeutic agents. Last, our data firmly establish relationships between high-grade serous carcinomas with solid, pseudoendometrioid, and transitional cell carcinoma-like morphological features (SET features). Excluding SET pattern tumors from the family of high-grade serous carcinoma might prevent affected patients or their families from being eligible for targeted treatment or screening programs.

Acknowledgement

Disclosure/conflict of interest

The authors declare no conflict of interest.

References

1 Risch HA, McLaughlin JR, Cole DEC, *et al.* Prevalence and penetrance of germline *BRCA1* and *BRCA2* mutations in a population series of 649 women with ovarian cancer. Am J Hum Genet 2001;68:700–710.

2 Press JZ, De Luca A, Boyd N, *et al.* Ovarian carcinomas with genetic and epigenetic *BRCA1* loss have distinct molecular abnormalities. BMC Cancer 2008;8:17.

3 Husain A, He G, Venkatraman ES, *et al.* BRCA1 upregulation is associated with repair-mediated resistance to cis-diamminedichloroplatinum(II). Cancer Res 1998;58:1120–1123.

4 Yuan SS, Lee SY, Chen G, *et al.* BRCA2 is required for ionizing radiation-induced assembly of Rad51 complex in vivo. Cancer Res 1999;59:3547–3551.

5 Ben David Y, Chetrit A, Hirsh-Yechezkel G, *et al.* Effect of *BRCA* mutations on the length of survival in epithelial ovarian tumors. J Clin Oncol 2002;20:463–466.

6 Boyd J, Sonoda Y, Federici MG, *et al.* Clinicopathologic features of *BRCA*-linked and sporadic ovarian cancer. JAMA 2000;283:2260–2265.

7 Audeh MW, Carmichael J, Penson RT, *et al.* Oral poly(ADP-ribose) polymerase inhibitor olaparib in patients with *BRCA1* or *BRCA2* mutations and recurrent ovarian cancer: a proof-of-concept trial. Lancet 2010;376:245–251.

8 Tutt A, Robson M, Garber JE, *et al.* Oral poly(ADP-ribose) polymerase inhibitor olaparib in patients with *BRCA1* or *BRCA2* mutations and advanced breast cancer: a proof-of-concept trial. Lancet 2010;376:235–244.

BRCA1 and *BRCA2* morphologic patterns
636
RA Soslow *et al*

9 Fong PC, Yap TA, Boss DS, *et al.* Poly(ADP)-ribose polymerase inhibition: frequent durable responses in *BRCA* carrier ovarian cancer correlating with platinum-free interval. J Clin Oncol 2010;28:2512–2519.

10 Sato E, Olson SH, Ahn J, *et al.* Intraepithelial CD8+ tumor-infiltrating lymphocytes and a high CD8+/regulatory T cell ratio are associated with favorable prognosis in ovarian cancer. Proc Natl Acad Sci USA 2005;102:18538–18543.

11 Zhang L, Conejo-Garcia JR, Katsaros D, *et al.* Intratumoral T cells, recurrence, and survival in epithelial ovarian cancer. N Eng J Med 2003;348:203–213.

12 Hamanishi J, Mandai M, Iwasaki M, *et al.* Programmed cell death 1 ligand 1 and tumor-infiltrating CD8+ T lymphocytes are prognostic factors of human ovarian cancer. Proc Natl Acad Sci USA 2007;104:3360–3365.

13 Clarke B, Tinker AV, Lee CH, *et al.* Intraepithelial T cells and prognosis in ovarian carcinoma: novel associations with stage, tumor type, and *BRCA1* loss. Mod Pathol 2009;22:393–402.

14 Robey SS, Silva EG, Gershenson DM, *et al.* Transitional cell carcinoma in high-grade high-stage ovarian carcinoma. An indicator of favorable response to chemotherapy. Cancer 1989;63:839–847.

15 Gershenson DM, Silva EG, Mitchell MF, *et al.* Transitional cell carcinoma of the ovary: a matched control study of advanced-stage patients treated with cisplatin-based chemotherapy. Am J Obstet Gynecol 1993;168:1178–1187.

16 Kommoss F, Kommoss S, Schmidt D, *et al.* Survival benefit for patients with advanced-stage transitional cell carcinomas vs. other subtypes of ovarian carcinoma after chemotherapy with platinum and paclitaxel. Gynecol Oncol 2005;97:195–199.

17 Tisserand P, Fouquet C, Barrois M, *et al.* Lack of HIN-1 methylation defines specific breast tumor subtypes including medullary carcinoma of the breast and *BRCA1*-linked tumors. Cancer Biol Ther 2003;2:559–563.

18 Armes JE, Egan AJM, Southey MC, *et al.* The histologic phenotypes of breast carcinoma occurring before age 40 years in women with and without *BRCA1* or *BRCA2* germline mutations: a population-based study. Cancer 1998;83:2335–2345.

19 Lakhani SR, Gusterson BA, Jacquemier J, *et al.* The pathology of familial breast cancer: histological features of cancers in families not attributable to mutations in *BRCA1* or *BRCA2*. Clin Cancer Res 2000;6:782–789.

20 Wong EM, Southey MC, Fox SB, *et al.* Constitutional methylation of the *BRCA1* promoter is specifically associated with *BRCA1* mutation-associated pathology in early-onset breast cancer. Cancer Prev Res 2011;4:23–33.

21 The Cancer Genome Atlas Research Network. Integrated genomic analyses of ovarian carcinoma. Nature 2011;474:609–615.

22 Gilks CB, Ionescu DN, Kalloger SE, *et al.* Tumor cell type can be reproducibly diagnosed and is of independent prognostic significance in patients with maximally debulked ovarian carcinoma. Hum Pathol 2008;39:1239–1251.

23 Eichhorn JH, Young RH. Transitional cell carcinoma of the ovary: a morphologic study of 100 cases with emphasis on differential diagnosis. Am J Surg Pathol 2004;28:453–463.

24 Rubin SC, Benjamin I, Behbakht K, *et al.* Clinical and pathological features of ovarian cancer in women with germ-line mutations of *BRCA1*. N Engl J Med 1996;335:1413–1416.

25 Takahashi H, Behbakht K, McGovern PE, *et al.* Mutation analysis of the *BRCA1* gene in ovarian cancers. Cancer Res 1995;55:2998–3002.

26 Roh MH, Yassin Y, Miron A, *et al.* High-grade fimbrial-ovarian carcinomas are unified by altered p53, PTEN and PAX2 expression. Mod Pathol 2010;23:1316–1324.

27 Takahashi H, Chiu HC, Bandera CA, *et al.* Mutations of the *BRCA2* gene in ovarian carcinomas. Cancer Res 1996;56:2738–2741.

28 Werness BA, Ramus SJ, DiCioccio RA, *et al.* Histopathology, FIGO stage, and *BRCA* mutation status of ovarian cancers from the Gilda Radner Familial Ovarian Cancer Registry. Int J Gynecol Pathol 2004;23:29–34.

29 Lakhani SR, Manek S, Frederique Penault-Llorca F, *et al.* Pathology of ovarian cancers in *BRCA1* and *BRCA2* carriers. Clin Cancer Res 2004;10:2473–2481.

30 Boyd J, Sonoda Y, Federici MG, *et al.* Clinicopathologic features of *BRCA*-linked and sporadic ovarian cancer. JAMA 2000;283:2260–2265.

31 Logani S, Oliva E, Amin MB, *et al.* Immunoprofile of ovarian tumors with putative transitional cell (urothelial) differentiation using novel urothelial markers: histogenetic and diagnostic implications. Am J Surg Pathol 2003;27:1434–1441.

32 Wu R, Hendrix-Lucas N, Kuick R, *et al.* Mouse model of human ovarian endometrioid adenocarcinoma based on somatic defects in the Wnt/β-catenin and PI3K/Pten signaling pathways. Cancer Cell 2007;11:321–333.

33 Soslow RA. Histologic subtypes of ovarian carcinoma: an overview. Int J Gynecol Pathol 2008;27:161–174.

34 Köbel M, Kalloger SE, Baker PM, *et al.* Diagnosis of ovarian carcinoma cell type is highly reproducible: a Trans-Canadian study. Am J Surg Pathol 2010;34:984–993.